Scour depth model for grade-control structures

Ahmed M. A. Sattar, Karol Plesiński, Artur Radecki-Pawlik and Bahram Gharabaghi

ABSTRACT

Grade-control structures (GCS) are commonly used to protect fish habitat by preventing excessive river-bed degradation in mountain streams. However, flow over the GCS can cause localized scour immediately downstream of the weir. This paper aims to develop more accurate models for prediction of the maximum scour depth downstream of GCS, using a more extensive dataset and evolutionary gene expression programming (GEP). Three GEP models are developed relating maximum scour depth and various control variables. The developed models had the lowest error compared to available models. A parametric analysis is performed for further verification of the developed GEP model. The results indicate that the proposed relations are simple and can more accurately predict the scour depth downstream GCS.

Key words | evolutionary algorithms, gene expression programming, grade-control structures, parametric analysis, scour depth, uncertainty analysis

Ahmed M. A. Sattar
Department of Irrigation & Hydraulics, Faculty of Engineering,
Cairo University,
Giza,
Egypt

Karol Plesiński
Department of Hydraulics Engineering and Geotechnics,
Agricultural University of Cracow,
al. Mickiewicza 24/28, 30-059 Kraków,
Poland

Artur Radecki-Pawlik
Faculty of Civil Engineering,
Cracow University of Technology,
ul. Warszawska 24, 31-155 Kraków,
Poland

Bahram Gharabaghi (corresponding author)
Water Resources Engineering, School of Engineering,
University of Guelph,
Room 2417, Thornbrough Building, 50 Stone Road East, Guelph, Ontario,
Canada
N1G 2W1
E-mail: *bgharaba@uoguelph.ca*

INTRODUCTION

Grade-control structures (GCS) (Figure 1) are commonly prescribed to improve aquatic habitats in mountain streams by preventing excessive river-bed degradation (Veronese 1937; Mason & Arumugam 1985; Lenzi *et al.* 2003a; Muzzammil & Siddiqui 2009). GCS simulate alluvial river bed forms (riffles), do not require additional fish passage consideration, and naturally aerate flowing water over the weir (Farhoudi & Smith 1985; Hassan & Narayanan 1985; Bormann & Julien 1991).

However, the flow over GCS can cause localized scour downstream of the weir, potentially leading to failure of the structure (e.g., Guven & Gunal 2008; Abou-Seida *et al.* 2012). The key factors influencing the scour process include upstream water head, weir height, tail water level, bed particle grain-size distribution, and particle density (Bormann & Julien 1991; Lenzi & Comiti 2003; Marion *et al.* 2004; Pagliara 2007; Goel & Pal 2009; Azamathulla 2012; Atieh *et al.* 2017). To ensure safe design of the GCS to withstand expected flood events would require models for site-specific accurate prediction of the maximum depth of scour. Such models have been historically developed based on a combination of typically small set of laboratory-scale experiment data and limited field surveys (e.g., Bormann & Julien 1991; Mossa 1998; D'Agostino & Ferro 2003; Lenzi & Comiti 2003; Marion *et al.* 2004; Pagliara *et al.* 2004; Meftah & Mossa 2006; Pagliara 2007; Pagliara & Palermo 2008; Guven 2011; Radecki-Pawlik 2013; Guan *et al.* 2016). However, Scurlock *et al.* (2012) showed that for most models, the available experimental data – used for model development – were

doi: 10.2166/hydro.2017.149

Figure 1 | GCS on the Krzczonowski stream, Poland.

not sufficient to yield reliable scour depths and that prediction errors can reach 300%.

Another major disadvantage in most of the previously developed GCS scour depth models is that they are based on regression analysis, which may not be able to capture the complex relationship between key factors. Machine learning techniques, including gene expression programming (GEP), however, have been recently used by many researchers for developing complex models as an efficient alternative to traditional regression and other machine learning methods (Sattar 2014a, 2014b, 2016a, 2016b; Gazendam *et al.* 2016; Sabouri *et al.* 2016; Sattar *et al.* 2016, 2017; Gharabaghi & Sattar 2017; Thompson *et al.* 2016).

Thus, this work aims to overcome many of the previous studies' shortcomings by collecting large-scale field scour data downstream GCS in Polish mountain streams that can complement the existing database of experimental and field measurements. Moreover, this study presents the novel application of GEP for development of a scour depth prediction model that is capable of predicting scour downstream structures with higher accuracy than previous regression-based models. In this study, we conducted field surveys of 17 scour holes downstream of GCS in two Polish streams to augment 248 existing experimental and field measurements from several published papers from studies around the globe to build a comprehensive database for model development using GEP. The control variables used as predictors include flow rate, GCS height and width, and bed material representative particle sizes. GEP is used to find optimum prediction models with the least error and the best fit. The prediction uncertainty of the developed GEP models is quantified and compared with those of existing equations, and a parametric analysis is performed for further verification of the developed GEP models.

MODELS FOR SCOUR DEPTH PREDICTION

Many historic studies used to predict the scour depth downstream GCS have used semi-analytical approaches; however, none of these models has proven to be sufficient for full description of the complex scour process and the related turbulent hydrodynamic factors. Bormann & Julien (1991) analyzed the jet diffusion and corresponding sediment incipient motion and developed a model with a simple equation that predicted the maximum scour depth. Their model has been modified by Stein & Julien (1994) to account for additional factors and provide more accurate predictions. Another similar model has been developed by Hoffmans (1998) based on the jet momentum dynamic approach. Chen & Hong (2001) performed complex analysis for the scour hole shape and proposed equations for maximum scour depth for uniform and graded sediment.

Another popular approach has been the development of empirical equations based on regression analysis using laboratory experimental and field survey data. Lenzi *et al.* (2003b) presented a summary of these historic models and highlighted major shortcomings, including insufficient representations for the complex scour process, dependency on various coefficients that are difficult to calculate, requirement for field calibration for model before application on a specific site, and presence of high degree of uncertainty in their results. One of the first empirical models for maximum scour depth downstream of GCS was developed by Mason & Arumugam (1985) and suggested a general form for a scour equation as:

$$D_m = K\frac{q^a u^b D_g^c \beta^d}{g^e d_s^f} - z_g \tag{1}$$

where a, b, c, d, e, f are exponents with different values (review of exponent values for different studies is available in Bormann & Julien 1991), k is a coefficient based on experimental results and a function of the tail water level, g is the gravitational acceleration, d_s is the effective grain diameter and taken as d_{90}, q is the unit discharge over the structure, U is the jet velocity across the structure, D_g is the head drop according to the structure, and β is the jet angle at bed impact (see Figure 2).

D'Agostino & Ferro (2004) proposed regression-based models for estimating the maximum scour depth downstream GCS with the following form:

$$\frac{D_m}{z_g} = 0.975\left(\frac{H_o}{z_g}\right)^{0.863} \tag{2}$$

and

$$\frac{D_m}{z_g} = 0.54\left(\frac{b}{z_g}\right)^{0.593}\left(\frac{H_o}{D_g}\right)^{-0.126}\left(\frac{d_{90}}{d_{50}}\right)^{-0.856}\left(\frac{b}{B}\right)^{-0.751} A_{50} \tag{3}$$

where b is the grade control structure width, H_o is the approaching flow depth, B is the channel width, d_{90}, d_{50} are the 90-th and 50-th percent finer bed sediment diameters, and A_{50} is a dimensionless number defined as:

$$A_{50} = \frac{Q}{bz_g\sqrt{gd_{50}(\Delta - 1)}} \tag{4}$$

where Q is the flow through the GCS, Δ is the sediment relative density.

Pagliara & Palermo (2008) investigated the effect of the rock sills on scour geometry downstream GCS and carried out investigation to reach the following formula:

$$\frac{D_m}{z_g} = 2.45e^{\frac{0.06Q}{bz_g\sqrt{gd_{90}(\Delta - 1)}}} \tag{5}$$

Laucelli & Giustolisi (2011) presented several empirical models for scour prediction using evolutionary polynomial regression applied on field and laboratory measurements. The following equations have been presented:

$$\frac{D_m}{z_g} = e^{0.6437\sqrt{b/z_g}} \tag{6}$$

and

$$\frac{D_m}{z_g} = e^{0.1511\sqrt{A_{50}}+0.9555\left(H_o/H_o+z_g\right)} \tag{7}$$

and

$$\frac{D_m}{z_g} = e^{0.4787\sqrt{\frac{H_o/z_g}{b/B}}+0.024\left(\frac{d_{90}}{d_{50}}\right)^2} \tag{8}$$

and

$$\frac{D_m}{z_g} = e^{0.2168\sqrt{b/z_g}+0.1047\sqrt{A_{50}}+0.7646\left(H_o/H_o+z_g\right)^2} \tag{9}$$

Using the same non-dimensional parameters, Guven (2011) utilized the non-linear regression in addition to

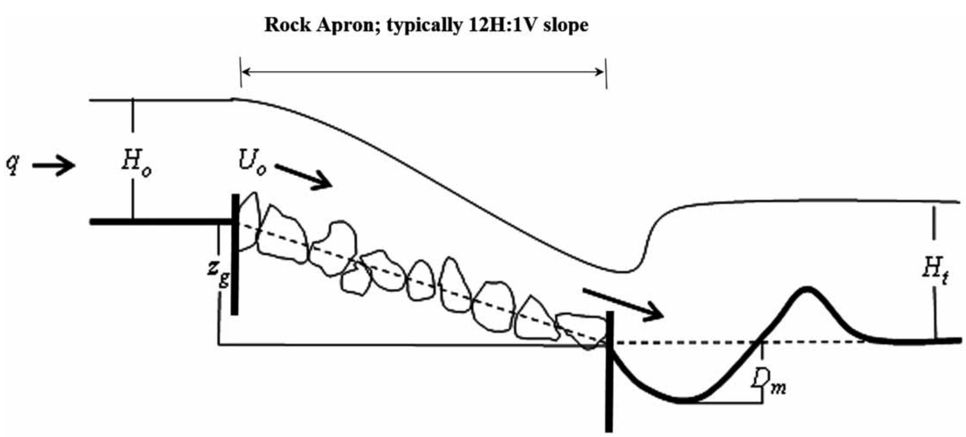

Figure 2 | Scour behind GCS.

parameter optimization to develop the following model:

$$\frac{D_m}{z_g} = 0.193(A_{50})^{0.838}\left(\frac{H_t}{z_g}\right)^{0.931}\left(\frac{d_{90}}{d_{50}}\right)^{1.217} \tag{10}$$

where H_t is the tail water depth downstream of the GCS. Equations for scour depth prediction from Equations (2)–(10) have some advantages over the equation form in Equation (1). They account for non-uniform bed sediment through the term d_{90}/d_{50}, and the 3D flow owing to channel contraction through the term b/B. Moreover, these equations can be used to predict scour depth even if it is larger than the structure height, which is a major limitation of Equation (1).

MATERIALS AND METHODS

Site selection

Many rivers in Poland are regulated using dams, bed sills, and low-head GCSs. These structures lead to channel bed stabilization and prevent successive erosion, where a dynamic equilibrium forms between bed scouring and aggradation. In this study, a detailed field survey for 17 scour hole downstream GCS was carried on two mountainous streams in Poland during the period from 2009 to 2015. The Porębianka River is 15.4 km long with a catchment area of 72 km^2 and the Poniczanka River is 10.2 km long with a catchment area of 10.3 km^2, both located in the southern part of Poland in the Gorce Mountains (Figure 3). These mountainous rivers begin at the Obidowa peak (1,000 m a.s.l.) and rapidly drop elevations to below 500 m a.s.l. at the outlet.

Grade-control structures

A total of 25 GCS have been constructed on the Porębianka River to stabilize the channel bed from Mszana Dolna town to Niedźwiedź village. These GCS are similar in construction and consist of two sheet pilings spread a distance of 12 to 24 m apart with elevation drops ranging from 1 to 2 m resulting in angles of inclination of 3° and 5°. The area between the sheet pilings is filled with boulders of 0.9 m average diameter, also known as the sloping rock apron (Figure 2). In the central part of the upper and lower sheet pilings, the crown elevation of the sheet pile at the centerline of the river is reduced about 20 cm on a 4 m length in order to concentrate the flow of water during the low flows for ease of fish migration.

Out of a total of 25 scour holes, 17 were chosen after careful inspection, such that the bottoms of all the holes were armored by coarse material with an average size equivalent to the largest found in the stream (Figure 4). The boulders and cobbles at each hole's bottom were tight and adjoined to each other with no clasts on their surface or fine sediment. This ensures that the scour hole has reached the dynamic equilibrium between water-sediment discharges and its dimensions. For each scour hole, the GCS height and the maximum scour depth were measured from surveyed profiles (Figure 5).

GEP for model development

The functional relationships between the scour depth and related parameters can be determined by regression analysis or machine learning methods (e.g., artificial neural networks (ANNs), GEP). Although ANNs are successfully used in hydrology and water resources models, many studies have proven that GEP can be useful in many hydraulic engineering applications (e.g., Guven & Gunal 2008; El Hakeem & Sattar 2015; Najafzadeh & Sattar 2015; Sattar & Gharabaghi 2015; Sattar 2016a, 2016b; Sattar et al. 2016; Thompson et al. 2016).

As described in Sattar (2014a), GEP uses a random distribution of functions and terminals as chromosome genes to create 'parents'. The parent passes along its own genetic information to generate offspring. High-performing genetic operators (mutations and crossover) are used to yield offspring, which are adapted to the environment with greater fitness and with a higher chance of survival; the offspring is a better fit than the previously un-fit parent. The criterion of fitness of the offspring is evaluated based on its ability to achieve a value within a pre-determined error of the correct value of the function. This evolutionary strategy allows GEP to identify an optimal offspring, without preventing the evolution of the next generation. The fitness function of a program, f_i, is defined in the following equation where the

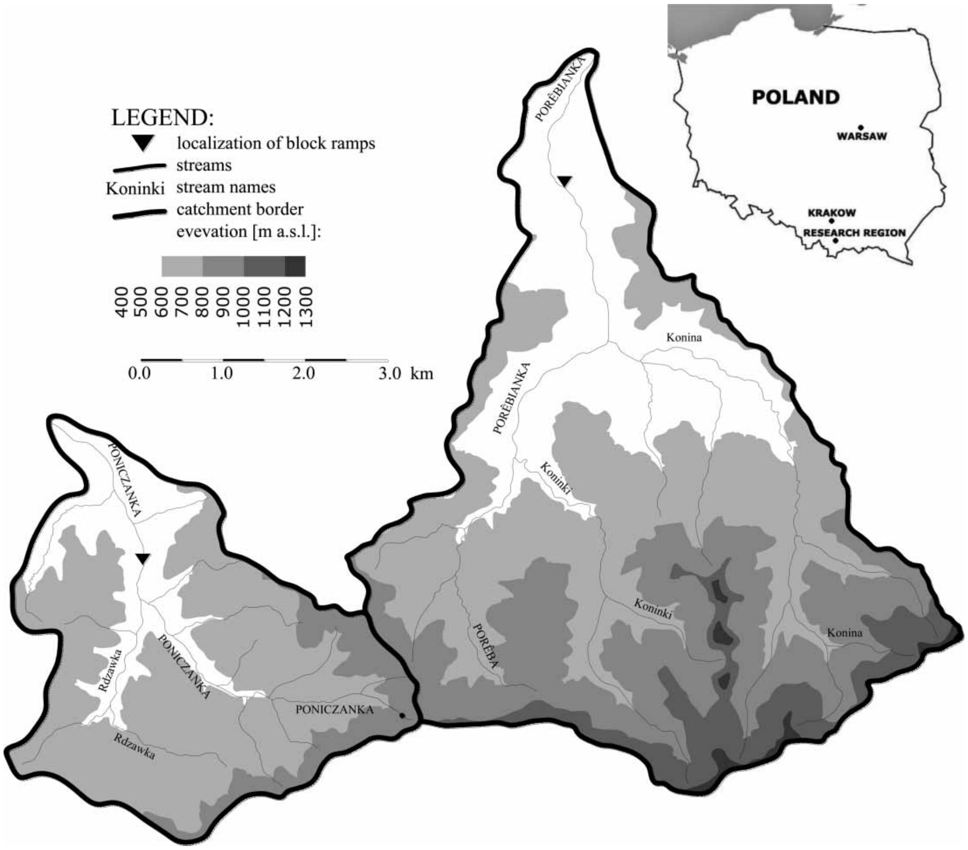

Figure 3 | Location of the Porębianka and Poniczanka River watersheds, Poland.

Figure 4 | The scour hole below block ramp on Porębianka stream, Poland.

error used is the root relative squared error (RRSE).

$$f_i = \frac{1,000}{1 + RRSE_i} \tag{11}$$

Equation (11) is used to determine the root relative square error RRSE of an individual program i (i-the offspring).

$$RRSE_i = \sqrt{\frac{\sum_{j=1}^{n}\left(P_{(ij)} - T_j\right)^2}{\sum_{j=1}^{n}\left(T_j - \bar{T}\right)^2}} \tag{12}$$

where $P_{(ij)}$ is the value predicted by the program i for fitness case j, T_j is the target value for fitness case j, $\bar{T} = 1/n\sum_{j=1}^{n} T_j$, and n is the number of samples. The RRSE ranges from 0 to infinity, with zero corresponding to a perfect fit (ideal). Genetic mutations are the main essence of genetic evolution in GEP and can be described in seven forms (Ferreira 2001). The GEP code developed by Radi & Poli (2002) has been utilized in this study.

The following procedure was used to develop the GEP models:

1. An initial set of control variables is chosen as terminals for GEP.
2. The initial work environment is set for GEP by defining the chromosome architecture (number of genes, head size, functions) and mutation rates.
3. GEP randomly formulates the chromosomes of the parent program and implements genetic operators to yield many first-generation offspring.
4. GEP uses the fitness criteria to find the fittest offspring. This offspring represents the solution to the problem in the first generation.
5. GEP considers the selected offspring the new parent and implements genetic operators to yield many second-generation offspring.
6. GEP evolution continues per steps 3, 4, and 5 until the specified program fitness is met.
7. The final GEP model (the fittest offspring of generation i) is scored on a set of performance indicators. These indicators are the square of the Pearson product moment correlation coefficient (R^2), the relative absolute error (RAE), coefficient of efficiency (E_{sn}), and index of agreement (D).

The indicators are calculated by the following equations:

$$R_i^2 = \left(\frac{1/n \sum_{j=1}^{n} (T_j - \bar{T})(P_{(ij)} - \bar{P})}{\sqrt{\sum_{j=1}^{n} (T_j - \bar{T})^2 / n} \sqrt{\sum_{j=1}^{n} (P_{(ij)} - \bar{P})^2 / n}} \right)^2 \tag{13}$$

$$RAE_i = \frac{\sum_{j=1}^{n} |P_{(ij)} - T_j|}{\sum_{j=1}^{n} |T_j - \bar{T}|} \tag{14}$$

$$E_{sn} = 1 - \frac{\sum_{i=1}^{n} (\mathrm{T}_i - \mathrm{P}_i)^2}{\sum_{i=1}^{n} (\mathrm{T}_i - \bar{\mathrm{T}})^2} \tag{15}$$

$$D = 1 - \frac{\sum_{i=1}^{n} (\mathrm{T}_i - \mathrm{P}_i)^2}{\sum_{i=1}^{n} (|\mathrm{P}_i - \bar{\mathrm{T}}| + |\mathrm{T}_i - \bar{\mathrm{T}}|)^2} \tag{16}$$

where $\bar{P} = 1/n \sum_{j=1}^{n} P_j$.

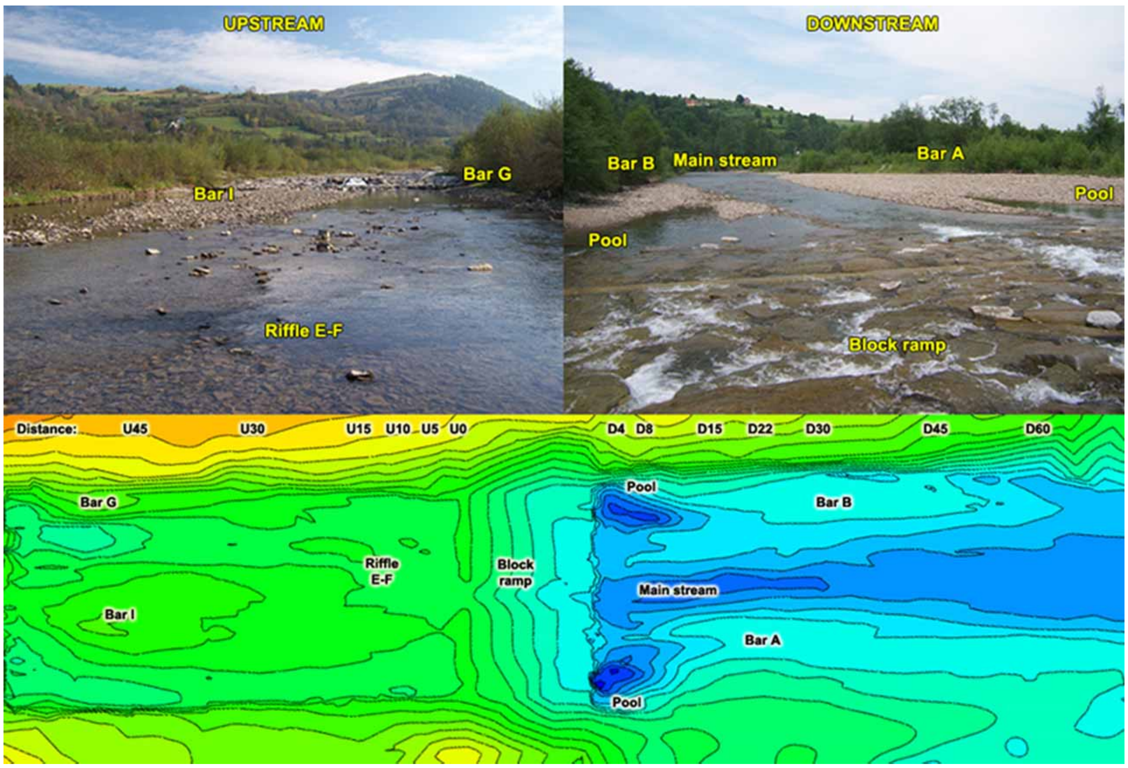

Figure 5 | Bathymetry of the scour hole below block ramp on Porębianka stream, Poland.

Validation of developed GEP models

Once the final models have been chosen, their performance with the testing data subset can be used for model validation. In this study, validation measures (Sattar 2014a, 2014b) are adopted. Of the gradients of the regression line through the origin for the predicted versus observed values (k), or for the observed versus predicted values (k'), at least one should be close to 1.

$$k = \frac{\sum_{i=1}^{n}(T_i \times P_i)}{P_i^2} \quad \text{or} \quad k' = \frac{\sum_{i=1}^{n}(T_i \times P_i)}{T_i^2}. \tag{17}$$

Additionally, the coefficient of determination for the regression lines through the origin m and n should be less than 0.1.

$$m = \frac{(R^2 - R_O^2)}{R^2} \text{ and } n = \frac{(R^2 - R_O'^2)}{R^2} \tag{18}$$

Moreover, the cross-validation coefficient R_m should satisfy:

$$R_m = R^2 \times \left(1 - \sqrt{|R^2 - R_O^2|}\right) > 0.5 \tag{19}$$

where the squared correlation coefficients through the origin between the predicted and observed values R_O^2 and between the observed and predicted values $R_O'^2$ are calculated from:

$$R_O^2 = \frac{1 - \sum_{i=1}^{n} P_i^2 (1-k)^2}{\sum_{i=1}^{n}(P_i - \bar{P})^2} \text{ and } R_O'^2 = \frac{1 - \sum_{i=1}^{n} T_i^2 (1-k')^2}{\sum_{i=1}^{n}(T_i - \bar{T})^2} \tag{20}$$

Uncertainty analysis of GEP models

The uncertainties of influencing parameters have to be included since this could affect the scour depth. A source of uncertainty in the model predictions is due to the sacristy of real data from large streams; therefore, a quantitative assessment of the models' stochastic character is presented in this section. The Monte Carlo simulation (MCS) (Sattar 2014a), is used to determine the uncertainty in pond temperature, due to uncertainty in the model's input parameters. These inputs are considered independent, as long as random sampling can be utilized without parameter combinations occurring and the output distribution tails are not affected; this can be assumed because the input parameters are known to be uncorrelated. The probability density function (PDF) is determined using distribution fitting, which relies on various input parameters and utilizing the complete available field and laboratory datasets. Optimal distributions are those with the highest scores in fitting tests, and are found to be generalized extreme value distribution. To conduct the MCS analyses, 250,000 runs are used. This number of MCS runs produced a converged variance for GEP models' output (Sattar 2014b). For each MCS run, the deterministic GEP model is used to obtain a single outcome. Thus, 250,000 outcomes are calculated for each of the input parameters and the uncertainty of these parameters is calculated as:

$$\text{Uncertainty }\% = \frac{100 \times \text{MAD}}{\text{Median(P)}} \tag{21}$$

According to Sattar (2014b), the mean absolute deviation (MAD) can be used to measure uncertainty in physical science and can be calculated as:

$$\text{MAD} = \frac{1}{250{,}000} \sum_{i=1}^{250{,}000} |\text{P}_\text{i} - \text{Median(P)}| \tag{22}$$

The uncertainty analysis defines the individual prediction error as $e_j = P_j - T_j$. The calculated prediction errors for the entire dataset are used to calculate the mean and standard deviation of the prediction errors as $\bar{e} = \sum_{j=1}^{n} e_j$ and $S_e = \sqrt{\sum_{j=1}^{n}(e_j - \bar{e})^2 / n - 1}$, respectively. A negative mean value indicates that the prediction model underestimated the observed values, and a positive value indicates that the equation overestimated the observed values. Using the values of $\bar{e}$ and S_e, a confidence band can be defined around the predicted values of an error using Wilson score method without continuity correction (Newcombe 1998); the use of $\pm 1.96\ S_e$ yields an approximately 95% confidence band.

Sensitivity analysis of GEP models

A sensitivity analysis was employed in order to identify which variables have more influence on the dimensionless scour depth downstream GCS. To investigate sensitivity, all input variables are assigned a fixed value and one variable is perturbed. The perturbation of this variable can be from 1% to 10% of its original value and helps determines the sensitivity of this variable and its influence on the GEP solution compared to other variables. Further, the marginal sensitivity coefficient is determined as (Sabouri et al. 2013; Robertson et al. 2015):

$$S_c = \frac{\Delta\varnothing}{\Delta E^*} \tag{23}$$

where $S_c =$ the marginal sensitivity coefficient, $\Delta\varnothing =$ the change in GEP prediction, and $\Delta E^* =$ the change in the parameter. Normalizing the parameters indicates the percent change in the objective function for a 10% change in each individual parameter. The marginal sensitivity coefficients were normalized to establish a basis of comparison:

$$S_n = S_c \frac{E^*}{\varnothing} \tag{24}$$

where S_n is the normalized sensitivity coefficient, $E^* =$ the expected value of the perturbed parameter, and $\varnothing =$ the expected solution. Higher normalized sensitivity coefficient implies higher sensitivity of the model to a specific parameter and vice versa. Moreover, the sign of the normalized sensitivity coefficient determines the gradient of change of solution with the increase in a specific parameter, i.e., when there is a positive sign, this means that the model prediction for scour depth increases with the increase in this parameter.

RESULTS AND DISCUSSION

Scour depth database

In this study, a comprehensive database of 265 scour depth measurements are compiled. These measurements include small GCS (Veronese 1937; D'Agostino & Ferro 2004), medium GCS (Bormann & Julien 1991) and large GCS on actual streams (Falciai & Giacomin 1978; D'Agostino 1994). The database includes 17 field measurements conducted in this study for large GCS in Polish streams. The database includes measurements of scour hole maximum depth (D_m) and various related flow, sediment and structure geometry parameters, i.e., the flow discharge (Q), the jet thickness (H_o), and the jet velocity (U_o), tail water level (H_t), median bed sediment size (d_{50}), length of the GCS (L_g), height of the GCS (z_g), and angle of inclination of the GCS downstream face (α_g). Falciai & Giacomin (1978) carried out 29 field measurements (Table 1) for scour depth

Table 1 | Range of variables in the case of large-scale GCS scour experiments

Variable category	Variables	Veronese (1937)	Falciai & Giacomin (1978)	Bormann & Julien (1991)	This study (2016)	D'Agostino (1994)	D'Agostino & Ferro (2004)
Data points	265	33	26	66	17	11	112
Flow	Q (m^3/s)	0.01–0.04	6.60–182.70	0.26–2.25	20.0–65.0	3.98–3.98	0.01–0.04
	U_o (m/s)	0.34–0.65	0.50–2.80	0.88–4.65	1.25–3.20	1.00–1.20	0.38–0.85
	H_o (m)	0.04–0.13	0.79–3.96	0.09–1.19	0.67–.12	0.40–0.50	0.04–0.21
	H_t (m)	0.05–0.25	1.13–4.90	0.24–1.65	0.86–1.56	0.50–0.70	0.08–0.44
Sediment	d_{50} (mm)	9.1–36.2	19.0–100.0	0.30–0.45	40.0–50.0	60	4.1–11.5
	d_{90} (mm)	9.1–36.2	37.0–117.0	1.58–1.71	58.0–69.0	60	7.0–17.6
GCS	L_g (m)	–	–	–	12.0–24.0	–	–
	z_g (m)	1.0–1.1	0.3–6.2	0.0–0.4	1.0–2.0	0.6–1.4	–
	α_g (°)	–	–	18–90	3.0–5.0	–	–
Scour hole	D_m (m)	0.1–0.2	0.40–3.50	0.10–1.52	0.15–2.30	0.3–0.7	0.045–0.3

downstream GCS in several rivers in the Tuscan Apennines in Italy with width from 5 to 20 m.

The unit discharges had a range from 1.2 to 13.4 m^2/s, the mean sediment diameter d_{50} from 19 to 100 mm, and the height of the GCS had a range from 0.3 to 6.2 m. The measured scour depth had a minimum value of 0.4 m and a maximum value of 3.5 m. The maximum scour depth data measured in the current study are from Porebianka and Poniczanka Rivers in Poland. The width of the rivers ranges from 8 to 12 m. The unit discharge has a range of 1 to 4.75 m^2/s, the jet velocity has a minimum value of 1.25 m/s and a maximum value of 3.2 m/s. The maximum measured scour depth ranges from 0.15 to 2.3 m. Table 2 presents the statistical parameters used in the study, which include maxima, minimum, average, and standard deviation.

Key factors affecting scour depth

D'Agostino & Ferro (2004) gave the variables affecting the scour downstream GCS due to the erosive action of water as $D_m = f(d_{50}, d_{90}, \Delta, g, Q, H_t, z_g, b, B, v, H_o)$. Using the Buckingham pi-theorem, they expressed this relation in terms of dimensionless parameters as:

$$\frac{D_m}{z_g} = f\left(\frac{b}{z_g}, \frac{H_t}{D_g}, \frac{d_{90}}{d_{50}}, \frac{b}{B}, A_{50}\right) \tag{25}$$

The equation above shows that the dimensionless scour downstream GCS depends on the GCS parameters b/z_g, channel parameters H_t/D_g, b/B, and sediment non-uniform coefficient d_{90}/d_{50}. Three GEP-based models were developed using different combinations of the above predictive parameters, as shown in Table 3. The effect of bed sediment non-uniformity was tested by excluding the parameter d_{90}/d_{50}, while the effect of the GCS was tested by excluding the parameter b/z_g. Using each parameter combination, the GEP model runs with an evolutionary mode until the fittest model is developed.

No strong correlation or interdependency was found among the predictor variables, thus eliminating the problems that could arise in analysis from exaggerating the strength of the relations between variables. The experimental database was divided into training and testing subsets. Several combinations were considered and the selection was made such that the main statistical descriptive parameters (mean and standard deviation) of both the training and testing subsets were consistent. Of the 265 values, 198 (75%) were used to develop the models, and 67 (25%) were used to test the models developed by using the GEP.

Developed GEP models

The best GEP models are obtained using the procedure specified in Sattar (2016c) with the optimal parameter settings shown in Table 4. It is to be noted that the optimal GEP parameters for this study might not be the optimum for other problems depending on the complexity of the input data. The following GEP models for the prediction of scour downstream GCS had high scores and low prediction errors.

GEP-1 model can be written as:

$$\frac{D_m}{z_g} = 0.0416A_{50} - 0.016\left(\frac{H_t}{z_g}\right)^2 - 0.014\frac{H_t}{z_g} + 0.194\frac{d_{90}}{d_{50}} \tag{26}$$

Table 2 | Statistical measures for the dataset utilized in this study

	Flow					Sediment		GCS			Scour hole
Variable	Q (m^3/s)	q ($m^3/s/m$)	U_o (m/s)	H_o (m)	H_t (m)	d_{50} (mm)	d_{90} (mm)	L_g (m)	z_g (m)	α_g (°)	D_m (m)
Minimum	0.26	0.29	0.57	0.09	0.14	0.30	1.58	12	0.05	4.77	0.05
Average	9.90	1.10	2.29	0.50	0.70	14.58	18.84	18	1.02	52.57	0.50
Maximum	182.70	13.40	4.45	3.96	5.00	100.0	109.0	24	6.20	89.95	3.50
Standard deviation	26	1.82	1.04	0.66	0.87	1.82	23.30	–	1.43	32.42	0.55

Table 3 | Input parameter combination used to predict scour hole depth

Model	Equation number	Input parameters to predict scour	Data type
Pagliara & Palermo (2008)	(5)	A_{50}	Laboratory data
D'Agostino & Ferro (2004)	(2)	$\frac{H_t}{D_g}$	Laboratory data
	(3)	$\frac{b}{z_g}, \frac{H_t}{D_g}, \frac{d_{90}}{d_{50}}, A_{50}$	
Laucelli & Giustolisi (2011)	(6)	$\frac{b}{z_g}$	Field and laboratory data
	(7)	$\frac{H_t}{D_g}, A_{50}$	
	(8)	$\frac{b}{z_g}, \frac{H_t}{D_g}, \frac{d_{90}}{d_{50}}$	
	(9)	$\frac{b}{z_g}, \frac{H_t}{D_g}, \frac{d_{90}}{d_{50}}, A_{50}$	
Guven (2011)	(10)	$\frac{H_t}{D_g}, \frac{d_{90}}{d_{50}}, A_{50}$	Laboratory data
GEP (this study)	(26)	$\frac{H_t}{D_g}, \frac{d_{90}}{d_{50}}, A_{50}$	Field and laboratory data
	(27)	$\frac{H_t}{D_g}, A_{50}$	
	(28)	$\frac{b}{z_g}, \frac{H_t}{D_g}, \frac{d_{90}}{d_{50}}, A_{50}$	

GEP-2 model is as follows:

$$\frac{D_m}{z_g} = \left(\frac{H_t}{z_g}\right)^{0.33} (A_{50})^{0.11} - 0.47\frac{H_t}{z_g} + 0.04A_{50} \tag{27}$$

Table 4 | Optimum parameter settings for GEP models

Parameter	Optimal setting
Number of generations	15,000
Number of chromosomes	40
Number of genes	3
Head size	3
Linking function	Multiplication
Fitness function error type	RRSE
Mutation rate	0.005
Inversion rate	0.1
One point recombination rate	0.3
Two point recombination rate	0.5
Gene recombination rate	0.1
Gene transposition rate	0.1
Function set	x, /, power
Random numerical constants	3
RNC mutation	0.001

GEP-3 model is as follows:

$$\frac{D_m}{z_g} = -0.39\left(\frac{z_g}{b}\right)^{0.25} + \left(\frac{H_t\,d_{90}}{z_g\,d_{50}}\right)^{0.25} + 0.039A_{50} - 0.28\left(\frac{H_t^2}{z_g\,b}\right) \tag{28}$$

In all of the GEP models, all of the parameters are non-dimensional. Table 5 gives a general overview of the GEP models developed to predict the dimensionless scour depth downstream GCS. The three GEP models performed well for both the training and testing datasets, with an average R^2 of 0.95 for training and of 0.90 for testing datasets. The error measures, RMSE and RAE show low values for training and testing datasets. The RMSE for GEP-01 and GEP-02 are 0.75 and 0.88, respectively, for training and testing sets. For GEP-03, error values for training and testing were lowest among the GEP models with values of 0.60 and 0.62 for training and testing sets, respectively. Similar trends are observed in the RAE calculated values. On the other hand, the E_{sn} and D show very good values for training and testing subsets with average values of 0.96, 0.99 for training subset and 0.90, 0.98 for testing subset.

Table 5 | Statistical performance of developed GEP prediction models

Model	Equation number	Data partitioning	R^2	RMSE	RAE	E_{sn}	D
Pagliara & Palermo (2008)	(5)	NA	0.48	2.75	0.62	0.30	0.82
D'Agostino & Ferro (2004)	(2)	NA	0.63	2.33	0.46	0.49	0.78
	(3)		0.75	2.26	0.59	0.53	0.81
Laucelli & Giustolisi (2011)	(6)	NA	0.68	2.41	0.79	0.46	0.70
	(7)		0.53	2.33	0.79	0.49	0.76
	(8)		0.76	2.71	0.75	0.32	0.53
	(9)		0.68	2.07	0.73	0.60	0.82
Guven (2011)	(10)	NA	0.71	33.54	3.71	103.43	0.27
GEP-01	(26)	Train	0.95	0.75	0.21	0.95	0.99
		Test	0.88	0.89	0.29	0.85	0.97
GEP-02	(27)	Train	0.95	0.77	0.25	0.94	0.99
		Test	0.88	0.88	0.30	0.86	0.97
GEP-03	(28)	Train	0.97	0.60	0.17	0.97	0.99
		Test	0.93	0.62	0.19	0.93	0.98

The Q-Q plot for the predicted versus the measured D_m/z_g for the three GEP models is shown in Figure 6. The figure shows the quality of prediction of the GEP models as they are applied on training and testing datasets. It is clear that the GEP-01 and GEP-02 models overestimated the scour depth for $D_m/z_g \leq 10$, while this is less noticeable in the GEP-03 model. Moreover, the terms A_{50}, H_t/z_g, d_{90}/d_{50} appeared as 'important predictors' in the developed GEP models. This is in agreement with the findings of most of the previous research, e.g., D'Agostino & Ferro (2004), Laucelli & Giustolisi (2011), and Guven (2011); while the term b/z_g appeared only in the GEP-03 model, similar to Laucelli & Giustolisi (2011).

Error analysis

Three different formulae for prediction of scour depth downstream large GCS have been developed. Table 5 shows the statistical measures of the developed GEP model prediction errors as compared to the historic models. The model developed by D'Agostino & Ferro (2004) and Laucelli & Giustolisi (2011) yielded the highest R^2 among all available models with value of 0.76, which is lower than that of all three developed GEP models. Pagliara & Palermo's (2008) model yielded the least R^2 with the capacity to represent only 50% of the scour data. The RMSE for the models of D'Agostino & Ferro (2004), Laucelli & Giustolisi (2011), and Pagliara & Palermo (2008) were close with an average value of 2.5, which is higher than that of the developed GEP models. On the other hand, Guven (2011) yielded the highest RMSE with a value of 33.5. Moreover, the results of E_{sn} and D indices for all available models were low and unacceptable ranging from 0.3 to 0.8 as compared to the GEP models which yielded high values of 0.95 on average. It is shown from the above discussion that the GEP models outperformed all available models on the scour dataset including large GCS. The GEP models can predict the target scour values with acceptable accuracy and less error than the available models.

Validation tests

As discussed before, the performance of developed models on testing data subsets was used to evaluate the prediction capability of the developed GEP models. Table 6 shows the validation criteria used and corresponding model performance, as calculated from Equations (17)–(20). Models have to satisfy some or all of the validation criteria. The gradients of the regression line for the predicted versus observed scour was close to 1 and within the recommended ranges of 0.85 to 1.15. This was accompanied by good values

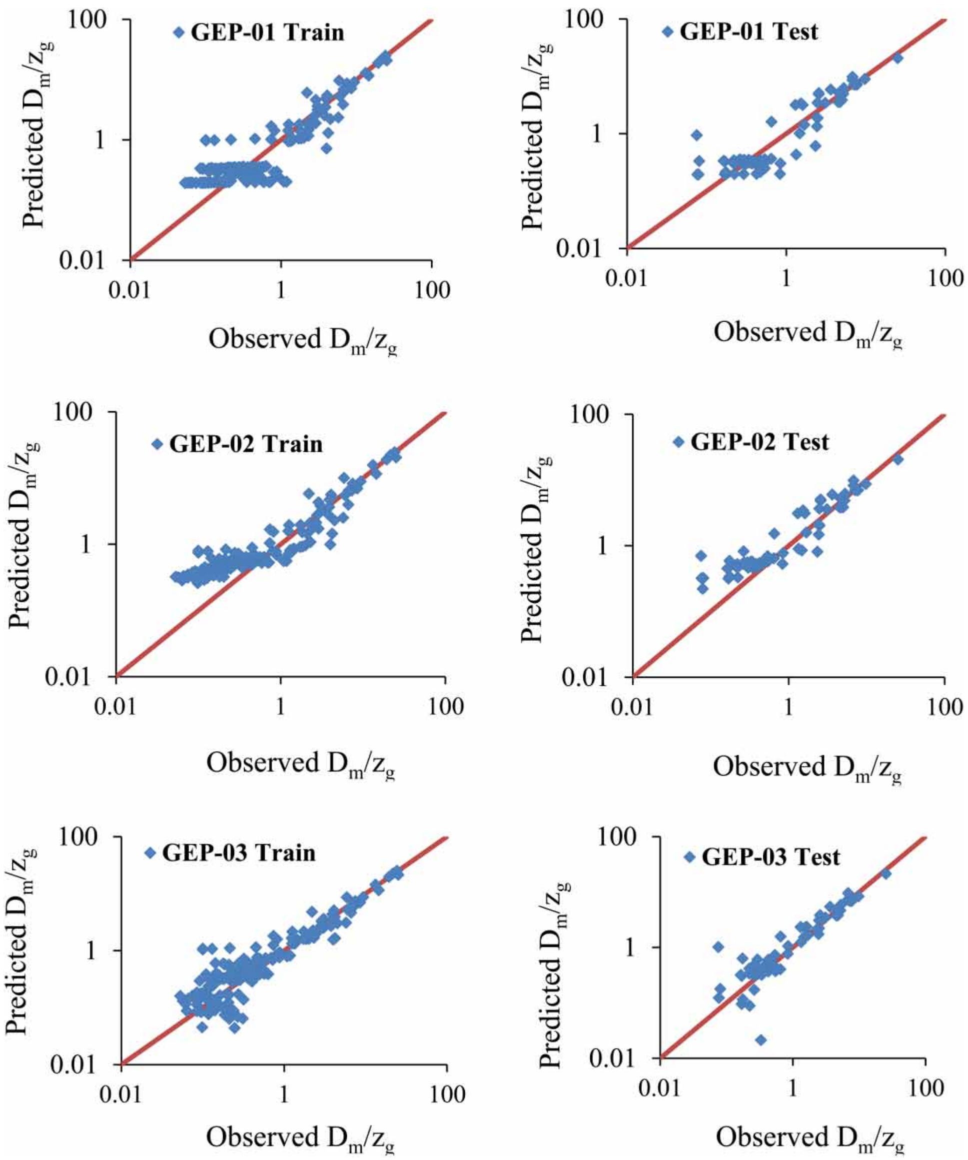

Figure 6 | Measured D_m/z_g versus that predicted by the three GEP models for Train/Test data.

Table 6 | Validation statistical measures for GEP prediction models (based on test dataset)

Model	R (R > 0.8)	K (0.85 < K < 1.15)	K′ (0.85 < K′ < 1.15)	M (m < 0.1)	N (n < 0.1)
GEP-01	0.95	0.92	0.88	−0.11	−0.10
GEP-02	0.97	1.11	0.72	−0.07	−0.03
GEP-03	0.94	0.83	0.96	−0.11	−0.13

for the coefficient of determination for the regression line with average values of −0.10. The condition of cross-validity was also satisfied for all developed models. This shows a good and accepted performance of the developed GEP models against test dataset.

Uncertainty analysis

The uncertainties in the predictions of the scour downstream large GCS are presented in Table 7 for the developed GEP models as well as the available empirical models. The uncertainty analysis is applied to the complete scour dataset used in this study. Table 7 shows the mean prediction errors of the various models, the width of the

Table 7 | Uncertainty estimates for GEP prediction models (based on test dataset)

Model	Equation number	Mean prediction error	Deviation of prediction error	Width of uncertainty band	95% prediction error interval
Pagliara & Palermo (2008)	(5)	−0.10	0.46	±0.90	0 to + 79
D'Agostino & Ferro (2004)	(2)	−0.04	0.31	±0.62	0 to + 18
	(3)	−1.05	0.59	±1.16	0 to + 234
Laucelli & Giustolisi (2011)	(6)	+0.40	0.53	±1.03	0 to + 46
	(7)	+0.37	0.53	±1.04	0 to + 51
	(8)	+0.30	0.55	±1.07	0 to + 70
	(9)	+0.41	0.50	±0.97	0 to + 35
Guven (2011)	(10)	−0.86	1.32	±2.59	0 to + 111
GEP-01	(26)	+0.01	0.27	±0.51	0 to + 10
GEP-02	(27)	+0.14	0.23	±0.44	0 to + 9
GEP-03	(28)	+0.04	0.27	±0.52	0 to + 5

uncertainty band and the 95% prediction interval error. All three GEP models have absolute mean prediction errors for scour depth downstream large GCS much less than those of the presented empirical models. The absolute mean prediction error for D'Agostino & Ferro (2004) and Laucelli & Giustolisi (2011) was four orders of magnitude larger than the GEP-01 and GEP-03 models. The deviation of prediction error for the GEP models was half that of the available empirical models with values of 0.25 and 0.6, respectively. According to the mean prediction error, GEP-01 and GEP-03 slightly overpredicted scour depth. This was the same observed behavior for the three empirical models of Laucelli & Giustolisi (2011), which showed overprediction, while the models of D'Agostino & Ferro (2004), Pagliara & Palermo (2008), and Guven (2011) showed underprediction for the scour depth. The uncertainty band width for the three GEP models is similar and ranged from ±0.44 to ±0.52. This range is half the range calculated for the other empirical models, which were from ±0.90 for the Pagliara & Palermo (2008) model to ±2.59 for Guven's (2011) model. Similarly, the lowest 95% confidence prediction error interval was observed for the GEP models. The GEP models had the lowest mean prediction error and the smallest uncertainty bands of all the compared models.

The results of the uncertainty associated with the predictions of the GEP models are shown in Table 8. The mean prediction for the scour depth was similar for GEP-01 and GEP-03 models with an average value of 1.25 m. The expected uncertainties in prediction of GEP-01 and GEP-02 models were similar with values of 41%, while the GEP-03 model yielded a lower prediction uncertainty of 24%. Uncertainties in the order or magnitude of 25–40% have been reported in the literature to be acceptable ranges for reliable models (Sattar 2014b). These uncertainty bands can be used together with GEP model predictions to provide an estimate for the maximum scour depth downstream large CGS.

Parametric analysis

In this section, a parametric analysis is performed on the developed GEP models to test their prediction behavior compared to the physics of the scour downstream GCS and how it is influenced by various input parameters. Beside being simple models, the developed GEP models show a clear combination of parameters that give them an advantage over existing grey-box machine learning methods. The average values of all parameters are used in prediction models and only one parameter (test parameter) is varied from a minimum value to a maximum value. Both the

Table 8 | Uncertainty analysis for GEP models outputs from MCS (results are based on 50,000 simulations)

Model	Median	Uncertainty %
GEP-01	1.33	44
GEP-02	1.67	41
GEP-03	1.22	24

chosen average and minimum/maximum values are from the parameter's range specified in Table 2.

Figure 7 shows the D_m/z_g versus d_{90}/d_{50} and H_t/z_g as calculated by the three GEP models and those of D'Agostino & Ferro (2004), Guven (2011), and Laucelli & Giustolisi (2011). The scour depth is directly proportional to the bed sediment gradation represented by the term d_{90}/d_{50}, where it increases with the increase in the term d_{90}/d_{50}.

This is consistent with the trends produced by the models of Guven (2011) and Laucelli & Giustolisi (2011) plotted in the same graph and is supported by the results of the sensitivity analysis shown in Table 9, where the d_{90}/d_{50} is one of the lower ranked influencing parameters on the scour depth.

This observation is consistent with previous experimental findings, where Guan *et al.* (2016) confirmed that experimental and field measurements of scour depth downstream GCS did not reveal pronounced effects for the sediment size in the scour process in rivers, and that its effect is much less than the effect of other parameters. Figure 7 also shows the change of the normalized scour depth versus the normalized tail water depth H_t/z_g. The developed GEP models show the same trend of change as the models of D'Agostino & Ferro (2004) and Laucelli & Giustolisi (2011). The increase in H_t/z_g results in a corresponding decrease in the normalized scour depth. This has been discussed and shown by Bormann & Julien (1991), who related the increase in the downstream water level to the increase in the flow diffusion length in the scour hole resulting in reducing the hydrodynamic forces acting on the stream bed. Again, the change in the scour depth is very small compared to a corresponding large change in the tail water depth. The normalized tail water depth had only 8 to 13% influence on the scour depth as calculated in Table 9. This behavior is also consistent with the findings of experimental and field measurements of Laucelli & Giustolisi (2011) and Scurlock *et al.* (2012), who found and confirmed that the effect of the tail water on the scour depth is minimal compared to other parameters.

According to results in Table 9, the parameter A_{50} showed the highest influence on the scour depth with 58% influence on GEP-02 and GEP-03 models, and increased to 80% in the GEP-01 model. The impact is clearly shown in Figure 8, where the increase in the term A_{50} caused a similar increase in normalized scour depth for the three GEP models in addition to D'Agostino & Ferro (2004) and Guven (2011) models.

Pagliara *et al.*'s (2004) experimental measurements showed that the high scour depths downstream GCS are related to high values of the A_{50} parameter and low

Table 9 | Sensitivity results of ANN and GEP prediction models

	S_n		
Attribute	**GEP-01**	**GEP-02**	**GEP-03**
A_{50}	+0.79	+0.58	+0.59
b/z_g	0.0	0.0	+0.11
H_t/z_g	−0.08	−0.13	−0.08
d_{90}/d_{50}	+0.25	0.0	+0.15

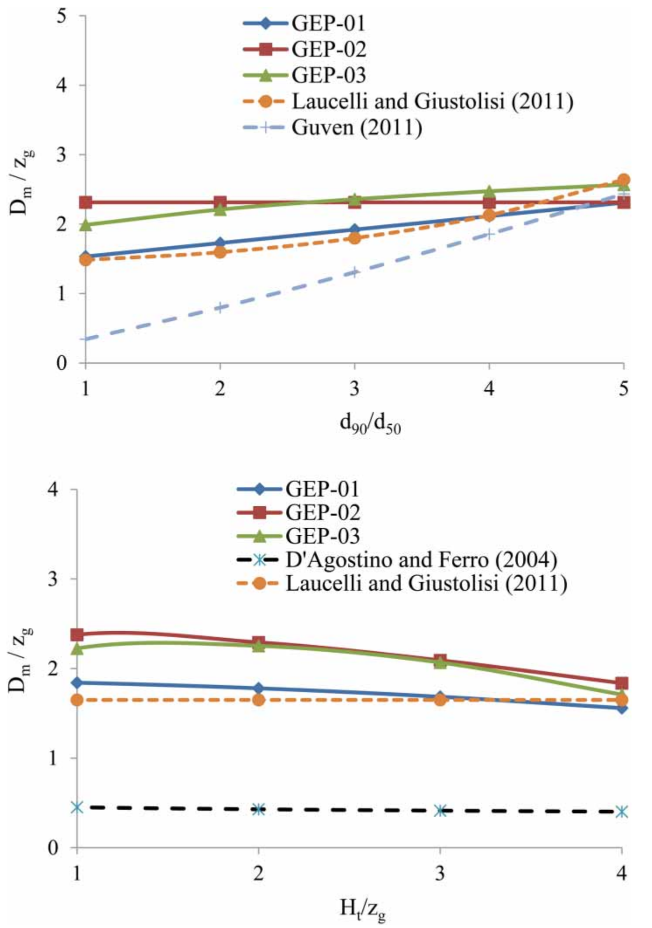

Figure 7 | D_m/z_g versus d_{90}/d_{50} and H_t/z_g as predicted by the GEP models and available models.

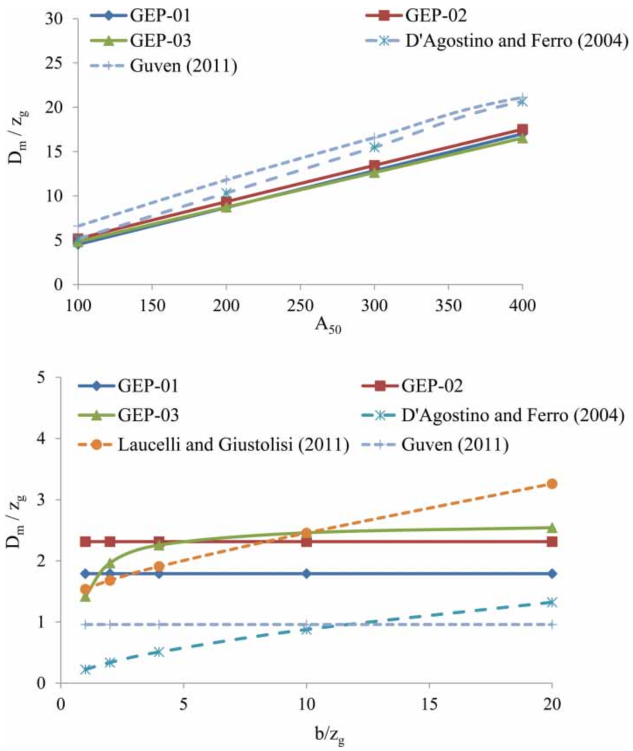

Figure 8 | D_m/z_g versus A_{50} and b/z_g as predicted by the GEP models and available models.

sediment concentrations. Following the A_{50} parameter, the normalized GCS width was ranked the second most influential parameter on the scour depth, as shown in Table 9.

The term b/z_g appeared only in the GEP-03 model with influence value of 11%. The normalized scour depth increased with the increase in b/z_g, as shown in Figure 8 for the GEP-03 model, which showed a similar trend to D'Agostino & Ferro (2004), Guven (2011), and Laucelli & Giustolisi (2011) models. This term accounts for the change in the stream width relative to the GCS. This change can trigger water circulation leading to a deflection and concentration for flow exiting the GCS ramp (Pagliara & Palermo 2008) resulting in an increase in the erosive water capacity and thus the increase in the scour depth.

CONCLUSIONS

The main goal of this paper was to develop more accurate models for prediction of the scour depth downstream of GCS to ensure safety and stability during flood flows. This is the first study of its kind to compile a comprehensive database of 265 scour depth measurements, consisting of both laboratory experiments and field surveys, to develop a more accurate model using GEP. The collected extensive dataset covers a wide range of the key factors influencing the scour process, including upstream water level, weir height, tail water level, and bed particle size distribution and particle density, therefore allowing the development of a superior model, compared to existing regression-based models, using GEP.

Selection criteria based on statistical measures and on external validation measures and the output of uncertainty analyses were used to select the best GEP models with the highest prediction accuracy and the least uncertainty. The prediction errors and uncertainties associated with the developed GEP models were significantly smaller than those associated with all of the existing empirical models. The root mean squared scour depth prediction error of the new GEP models dropped by 50% compared to the best of the existing empirical equations. The main reason for the superior performance of the new GEP models, compared with the existing empirical equations, is the use of the much larger/multi-scale dataset for the training of the new models and also the inclusion of the channel expansion parameter to enhance the performance of the new models.

Sensitivity analysis of the new GEP models revealed that the unit discharge has the highest influence on the scour depth, while the tail water depth and bed sediment size were found to have the least effect. The scour depth is directly proportional to the bed sediment gradation represented by the term d_{90}/d_{50} and indirectly proportional to H_t/z_g. The parameter A_{50} has the highest influence on the scour depth followed by the normalized GCS width as the second most influential factor.

ACKNOWLEDGEMENTS

The authors would like to acknowledge the funding and support of the Natural Sciences and Engineering Research Council of Canada (NSERC) and the University of Agriculture in Krakow, Department of Land Reclamation and Environmental Development (BM/4374/KIWiG/2016 – Project: 'The Researches for Young Scientists').

REFERENCES

Abou-Seida, M. M., Elsaeed, G. H., Mostafa, T. M. & Elzahry, E. F. 2012 Local scour at bridge abutments in cohesive soil. *Journal of Hydraulic Research* **50** (2), 171–180.

Atieh, M., Taylor, G., Sattar, A. M. & Gharabaghi, B. 2017 Prediction of flow duration curves for ungauged basins. *Journal of Hydrology* **545**, 383–394.

Azamathulla, H. M. 2012 Gene expression programming for prediction of scour depth downstream of sills. *Journal of Hydrology* **460**, 156–159.

Bormann, N. E. & Julien, P. Y. 1991 Scour downstream of grade-control structures. *Journal of Hydraulic Engineering* **117** (5), 579–594.

Chen, J. Y. & Hong, Y. M. 2001 Characteristics of check dam scour hole by free over-fall flow. *Journal of the Chinese Institute of Engineers* **24** (6), 673–680.

D'Agostino, V. 1994 Indagine sullo scavo a valle di opere trasversali mediante modello fisico a fondo mobile. (Survey of scour downstream structures using mobile bed model). *Energia Elettrica* **71** (2), 37–51 (in Italian).

D'Agostino, V. & Ferro, V. 2004 Scour on alluvial bed downstream of grade-control structures. *Journal of Hydraulic Engineering* **130** (1), 24–37.

El Hakeem, M. & Sattar, A. M. 2015 An entrainment model for non-uniform sediment. *Earth Surface Processes and Landforms*. DOI:10.1002/esp.3715.

Falciai, M. & Giacomin, A. 1978 Indagine sui gorghi che si formano a valle delle traverse torrentizie. *Italia Forestale Montana* **23** (3), 111–123.

Farhoudi, J. & Smith, K. V. H. 1985 Local scour profiles downstream of a hydraulic jump. *Journal of Hydraulic Research* **23** (4), 342–358.

Ferreira, C. 2001 Gene expression programming: a new adaptive algorithm for solving problems. *Complex Systems* **13** (2), 87–129.

Gazendam, E., Gharabaghi, B., Ackerman, J. & Whiteley, H. 2016 Integrative neural networks models for stream assessment in restoration projects. *Journal of Hydrology* **536**, 339–350.

Gharabaghi, B. & Sattar, A. M. 2017 Empirical models for longitudinal dispersion coefficient in natural streams. *Journal of Hydrology* (in press). DOI: 10.1016/j.jhydrol.2017.01.022.

Goel, A. & Pal, M. 2009 Application of support vector machines in scour prediction on grade-control structures. *Engineering Applications of Artificial Intelligence* **22** (2), 216–223.

Guan, D., Melville, B. & Friedrich, H. 2016 Local scour at submerged weirs in sand-bed channels. *Journal of Hydraulic Research* **54** (2), 172–184.

Guven, A. 2011 A multi-output descriptive neural network for estimation of scour geometry downstream from hydraulic structures. *Advances in Engineering Software* **42** (3), 85–93.

Guven, A. & Gunal, M. 2008 Genetic programming approach for prediction of local scour downstream hydraulic structures. *Journal of Irrigation and Drainage Engineering* **134** (2), 241–249.

Hassan, N. M. & Narayanan, R. 1985 Local scour downstream of an apron. *Journal of Hydraulic Engineering* **111** (11), 1371–1385.

Hoffmans, G. J. 1998 Jet scour in equilibrium phase. *Journal of Hydraulic Engineering* **124** (4), 430–437.

Laucelli, D. & Giustolisi, O. 2011 Scour depth modelling by a multi-objective evolutionary paradigm. *Environmental Modelling & Software* **26** (4), 498–509.

Lenzi, M. A. & Comiti, F. 2003 Local scouring and morphological adjustments in steep channels with check-dam sequences. *Geomorphology* **55** (1–4), 97–109.

Lenzi, M. A., Marion, A. & Comiti, F. 2003a Local scouring at grade-control structures in alluvial mountain rivers. *Water Resources Research* **39** (7), 1176.

Lenzi, M. A., Marion, A. & Comiti, F. 2003b Interference processes on scouring at bed sills. *Earth Surface Processes and Landforms* **28**, 99–110.

Marion, A., Lenzi, M. A. & Comiti, F. 2004 Effect of sill spacing and sediment size grading on scouring at grade-control structures. *Earth Surface Processes and Landforms* **29** (8), 983–993.

Mason, P. J. & Arumugam, K. 1985 Free jet scour below dams and flip buckets. *Journal of Hydraulic Engineering* **111** (2), 220–235.

Meftah, B. M. & Mossa, M. 2006 Scour holes downstream of bed sills in low-gradient channels. *Journal of Hydraulic Research* **44** (4), 497–509.

Mossa, M. 1998 Experimental study on the scour downstream of grade-control structures. In: *Proceedings of the 26th Convegno di Idraulica e Costruzioni Idrauliche*, Catania, Italy, September 3, pp. 581–594.

Muzzammil, M. & Siddiqui, N. A. 2009 A reliability-based assessment of bridge pier scour in non-uniform sediments. *Journal of Hydraulic Research* **47** (3), 372–380.

Najafzadeh, M. & Sattar, A. M. 2015 Neuro-fuzzy GMDH approach to predict longitudinal dispersion in water networks. *Water Resources Management* **29**, 2205–2219. doi:10.1007/s11269-015-0936-8.

Newcombe, R. G. 1998 Two sided confidence intervals for the single proportion: comparison of seven methods. *Statistics in Medicine* **17** (8), 857–872.

Pagliara, S. 2007 Influence of sediment gradation on scour downstream of block ramps. *Journal of Hydraulic Engineering* **133** (11), 1241–1248.

Pagliara, S. & Palermo, M. 2008 Scour control and surface sediment distribution downstream of block ramps. *Journal of Hydraulic Research* **46** (3), 334–343.

Pagliara, S., Hager, W. H. & Minor, H. E. 2004 Plunge pool scour in prototype and laboratory. In: *International Conference of Hydraulics of Dams and River Structures*, Tehran, Iran, pp. 165–172.

Radecki-Pawlik, A. 2013 On using artificial rapid hydraulic structures (RHS) within mountain stream channels: some exploitation and hydraulic problems. In: *Experimental and Computational Solutions of Hydraulic Problems* (P. Rowinski, ed.). GeoPlanet: Earth and Planetary Sciences, Springer Netherlands, pp. 101–115.

Radi, A. & Poli, K. 2002 *Genetic Programming Discovers Efficient Learning Rules for the Hidden and Output Layers of Feedforward Neural Networks*. Volume 1598 of the series Lecture Notes in Computer Science, pp. 120–134.

Robertson, B., Gharabaghi, B. & Hall, K. 2015 Prediction of breaking wave heights using artificial neural networks. *Coastal Engineering Journal* **57** (4). doi: 10.1142/S0578563415500187.

Sabouri, F., Gharabaghi, B., Mahboubi, A. A. & McBean, E. A. 2013 Impervious surfaces and sewer pipe effects on stormwater runoff temperature. *Journal of Hydrology* **502**, 10–17.

Sabouri, F., Gharabaghi, B., Sattar, A. & Thompson, A. M. 2016 Event-based stormwater management pond runoff temperature model. *Journal of Hydrology* **540**, 306–316.

Sattar, A. M. 2014a Gene expression models for the prediction of longitudinal dispersion coefficients in transitional and turbulent pipe flow. *Journal of Pipeline Systems Engineering and Practice* **5** (1), 04013011.

Sattar, A. M. 2014b Gene expression models for prediction of dam breach parameters. *Journal of Hydroinformatics* **16** (3), 550–571.

Sattar, A. M. 2016a Prediction of organic micropollutant removal in soil aquifer treatment system using GEP. *Journal of Hydrologic Engineering* **21** (9). DOI 10.1061/(ASCE)HE.1943-5584.0001372.

Sattar, A. M. 2016b A probabilistic projection of the transient flow equations with random system parameters and internal boundary conditions. *Journal of Hydraulic Research* **54** (3), 342–359. DOI: 10.1080/00221686.2016.1140682.

Sattar, A. M. 2016c Closure to 'Gene expression models for the prediction of longitudinal dispersion coefficients in transitional and turbulent pipe flow' by Ahmed M. A. Sattar. 2016. *Journal of Pipeline Systems Engineering and Practice* **7** (4). doi:10.1061/(ASCE)PS.1949-1204.0000254.

Sattar, A. M. & Gharabaghi, B. 2015 Gene expression models for prediction of longitudinal dispersion coefficient in streams. *Journal of Hydrology* **524**, 587–596.

Sattar, A., Gharabaghi, B. & McBean, E. 2016 Prediction of timing of watermain failure using gene expression models. *Water Resources Management* **30** (5), 1635–1651. DOI: 10.1007/s11269-016-1241-x.

Sattar, A. M. A., Gharabaghi, B., Sabouri, F. & Thompson, A. M. 2017 Urban stormwater thermal gene expression models for protection of sensitive receiving streams. *Hydrological Processes* **31** (13), 2317–2496. DOI: 10.1002/hyp.11170.

Scurlock, S. M., Thornton, C. I. & Abt, S. R. 2012 Equilibrium scour downstream of three-dimensional grade-control structures. *Journal of Hydraulic Engineering* **138**, 167–176.

Stein, O. R. & Julien, P. Y. 1994 Sediment concentration below free overfall. *Journal of Hydraulic Engineering* **120**, 1043–1059.

Thompson, J., Sattar, A., Gharabaghi, B. & Warner, R. 2016 Event-based total suspended sediment particle size distribution model. *Journal of Hydrology* **536**, 236–246. DOI: 10.1016/j.jhydrol.2016.02.056.

Veronese, A. 1937 Erosioni di fondo a valle di uno scarico. (Erosion downstream structures in drains). *Annal. Lavori Pubbl.* **75** (9), 717–726 (in Italian).

First received 6 December 2016; accepted in revised form 31 July 2017. Available online 15 September 2017